PII: S0032-3861(96)00717-3

Polymer Vol. 38 No. 8, pp. 1845–1856, 1997
© 1997 Elsevier Science Ltd
Printed in Great Britain. All rights reserved
0032-3861/97/$17.00+0.00

Effect of molecular weight on two-stage sorption in concentrated polystyrene–ethylbenzene solutions

P. H. Tang and C. J. Durning*
Department of Chemical Engineering, Materials Science and Mining, Columbia University, New York, NY 10027, USA

and C. J. Guo and D. DeKee
Department of Chemical Engineering, University of Sherbrooke, Sherbrooke, Quebec J1K 2R1, Canada
(Received 28 June 1995; revised 11 June 1996)

We examine the effect of polymer molecular weight on two-stage weight uptake kinetics in concentrated polymer solutions just below the glass transition. New results are reported for ethylbenzene sorption in two monodisperse polystyrenes ($M = 100\,000$ and $350\,000$). The two-stage sorption data were fitted with a linear model coupling diffusion and viscoelasticity. A data-fitting scheme is described, efficient enough for routine analysis of sorption data with small bench-top computers. Two dimensionless parameters, α and θ, and a collective diffusion coefficient, D, are determined from each two-stage sorption curve. α, proportional to the ratio of the shear and osmotic moduli of the mixture, is nearly constant over the entire concentration range examined, and is insensitive to molecular weight. The diffusion Deborah number, θ, decreases monotonically with ethylbenzene content, while D increases with ethylbenzene content, but no systematic changes in θ or D were found with molecular weight. These results support the view that two-stage sorption results from a coupling of diffusion to high-frequency viscoelastic modes, which are insensitive to polymer molecular weight. © 1997 Elsevier Science Ltd. All rights reserved.

(Keywords: non-Fickian diffusion; viscoelastic diffusion; two-stage sorption)

INTRODUCTION

Gradient diffusion† governs the relaxation of compositional and osmotic heterogeneities in a solution. Its understanding in concentrated polymer solutions is of great practical importance since it controls the outcome of many coating, drying and patterning processes. As a result, a great deal of basic work has been done on the subject. The observed behaviours include ordinary Fickian diffusion and a variety of non-Fickian or 'viscoelastic' effects[1–4], which are not fully understood at present. This work contributes by examining the influence of polymer molecular weight on a specific viscoelastic effect observed during sorption experiments.

An important observation was made by Vrentas and Duda[5] concerning the basic nature of viscoelastic diffusion. For diffusion experiments in which the local composition of the solution does not change too much, Vrentas and Duda correlated the appearance of viscoelastic effects with a diffusion Deborah number, θ, giving the ratio of a dominant relaxation time for the mixture, measured mechanically, to a characteristic diffusion time. They observed Fickian diffusion for θ either very large or very small. Non-Fickian effects occur when $\theta \sim O(1)$. The observation suggested a connection between non-Fickian diffusion and the viscoelasticity of the mixture, which is now widely recognized.

The details of this connection remain uncertain, however. Over the past decade, a number of authors have published continuum-level theories coupling osmotic and mechanical fields, and predicting non-Fickian diffusion in viscoelastic mixtures[6–9]. Unfortunately, these have not been tested thoroughly against experiment: only a few comparisons between data and theory have appeared[11–14]. Consequently there are still a number of basic issues to be resolved, including establishing what the dominant mechanisms are that couple osmotic and viscoelastic relaxation, and the role of glass state features.

This paper continues a programme[7,10–12] of comparisons between one of the simpler theories for viscoelastic diffusion[7] and isothermal sorption data in concentrated polymer solutions. Here, we examine the influence of polymer molecular weight on 'two-stage' sorption, a particular viscoelastic feature observed in 'differential' sorptions just below the glass transition[2,10–12]. We aim to determine if the terminal relaxation plays an important role in the two-stage process.

THEORY

Model for differential sorption

Gradient diffusion in concentrated polymer solutions is often studied by sorption. *Figure 1* shows the situation

* To whom correspondence should be addressed

† The terms 'collective diffusion' and 'cooperative diffusion' are often used in the literature. In binary mixtures the term 'mutual diffusion' is also applied

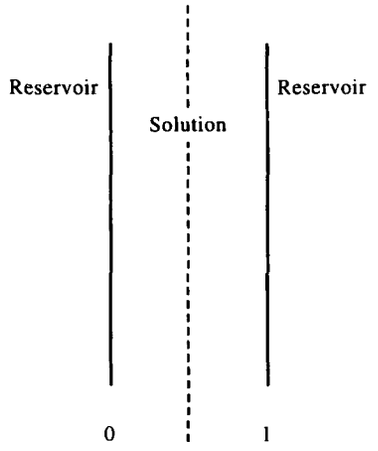

Figure 1 Schematic representation of one-dimensional sorption in a polymer solution

for experiments on a thin, unsupported film of the solution exposed to a reservoir of solvent on both sides. Initially ($t \leq 0^-$), the solution has solvent weight fraction $w^-{}_1$ dictated by equilibrium with the reservoir with solvent chemical potential $\mu^-{}_1$. At $t = 0$, the reservoir potential is increased to $\mu^+{}_1$. In response, solvent diffuses into the solution, causing an increase in its mass. As $t \to \infty$, a new equilibrium is established, with a solvent weight fraction $w^+{}_1$. One measures the mass of solvent absorbed during the relaxation to the new equilibrium. For 'differential' sorption, $\delta w \equiv (w^+{}_1 - w^-{}_1) \ll 1$, i.e. the initial and final equilibrium states are very close.

To model the response one needs a diffusion equation for the solvent concentration in the film. This follows from a continuity equation and a constitutive equation for the solvent flux. Durning and Tabor[7] derived the flux for a binary mixture with one viscoelastic component. We adopt their framework for analysis here.

In this development, volume additivity is assumed*. Consequently, local accumulation (depletion) of solvent during diffusion causes a dilation (compression) of polymer† and imposes a dynamic deformation history on the polymer, even in the absence of external tractions. This effect can change local state properties from the relaxed values. From this picture, Durning and Tabor derived an effective chemical potential for the fluid, μ_1, good for one-dimensional motions at constant total pressure:

$$\mu_1 = RTf(C,T,P) + \hat{V}_1\bar{V}_1\varphi_2 G(C) \times \int_{-\infty}^{t} \phi(C', t-t')\frac{\partial C'}{\partial t'}\mathrm{d}t' + \text{const.} \qquad (1)$$

The first term on the right gives the equilibrium or thermostatic potential, and the second gives a non-equilibrium, relaxing contribution from the memory of the mixture of the diffusion-induced deformation history. Here C is the solvent concentration, per unit volume of polymer. In the second term, $G(C)$ means the instantaneous shear modulus of the mixture and $\phi(C', t-t')$ means the relaxation function characterizing its linear viscoelastic mechanical response. $\hat{V}_i$ is the partial specific volume of component i, $\bar{V}_i$ is its molar volume and φ_2 is the polymer volume fraction.

Using μ_1 as a diffusion potential leads to a one-dimensional solvent flux, relative to the polymer, in the form

$$J_X = -D\frac{\partial C}{\partial X} - D'\frac{\partial}{\partial X}\int_{-\infty}^{t}\phi(t-t')\frac{\partial C}{\partial t'}\mathrm{d}t' \qquad (2)$$

with D being the 'polymer material' diffusion coefficient[15] and

$$D' = \frac{D\bar{V}_1}{RT}\frac{1}{w_2}\left(\frac{\partial f}{\partial w_1}\right)^{-1}\rho\hat{V}_1 G_0 \qquad (3)$$

Here $G_o \equiv G(C=0)$, w_i is the mass fraction of i and ρ is the mass density of the mixture.

Before analysis of the model, it is worth emphasizing a key assumption, that the local specific volume of the mixture always has the equilibrium value, as dictated by volume additivity. In another view[16], the system can violate volume additivity. Here, relatively rapid changes in composition can cause the specific volume of the mixture to deviate from the equilibrium value, triggering volume relaxation effects akin to those in temperature and pressure jump experiments on polymer glasses. Such effects can couple to diffusion, since unrelaxed volume affects the solvent chemical potential[17], but they are not considered in the present treatment.

Substituting equation (2) into the equation of continuity gives a linear† diffusion equation for C. Its solution requires boundary and initial conditions. For differential sorption, the former follow from the assumption of continuity of the fluid chemical potential at the solution/reservoir interfaces, and are conveniently specified at fixed reference locations in material coordinates[15]. The initial conditions correspond to the mixture being initially uniform and at equilibrium with the reservoir.

Durning and Tabor[7] developed an analytical solution for differential sorption for the case where ϕ corresponds to a Maxwell fluid. Billovits[12] employed a general Maxwell model for ϕ and used Laplace transformation to solve analytically for the transformed concentration; he converted into the time domain numerically to do data analysis. In this work, we report a completely different, numerical solution, more efficient for data analysis than either of the previous solutions.

The key to an effective solution is to introduce the memory function in lieu of the relaxation function in equation (2). This leads naturally to a different scaling of the diffusion equation than used by Durning and Tabor[7] and Billovits[12], and permits easier analysis of data.

Integration by parts of the second term on the right in equation (2) encourages the following scaled variables:

$$u = \frac{C - C^-}{C^+ - C^-} \quad x = \frac{X}{l} \quad s = \frac{t(D+D')}{l^2}$$

where C^- means the initial fluid concentration, C^+ means the final concentration and l is the dry film

* Volume additivity (no excess volume on mixing) implies constant partial specific volumes for the mixture components

† The details of local deformation of the polymer due to a local increase (decrease) in solvent content depend on the boundary constraints imposed on the sample, but it always has a dilational (compressional) component directly related to the change in composition when one assumes volume additivity

† For differential sorption the physical properties in equation (2) can be set constant, and the diffusion equation linearizes

thickness. The resulting dimensionless diffusion equation is

$$\frac{\partial u}{\partial s} = \frac{\partial^2 u}{\partial x^2} - \frac{\alpha}{\theta}\frac{\partial^2}{\partial x^2}\int_0^s m(s-s')u'\mathrm{d}s' \tag{4}$$

where $m = \tau(\partial\phi/\partial t')$ is a scaled memory function. The dimensionless parameters are

$$\alpha = \frac{D'}{D+D'} \qquad \theta = \frac{(D+D')\tau}{l^2} \tag{5}$$

The boundary conditions are

$$u - \frac{\alpha}{\theta}\int_0^s m(s-s')u'\mathrm{d}s' = 1-\alpha \quad \text{at } x = 0 \text{ and } 1 \tag{6}$$

and the initial conditions are

$$\left.\begin{aligned} u &= 0 \\ \frac{\partial u}{\partial s} &= 0 \end{aligned}\right\} \text{at } s = 0, \quad 0 < x < 1 \tag{7}$$

Restricting attention to the Maxwell model, where $m(s) = e^{-s/\theta}$, permits elimination of the integral from equation (4) by differentiating it with respect to s and back substituting. The resulting diffusion equation, a high-order partial differential equation (PDE), can be converted into a lower-order coupled system by transforming $u_1 = u$ and $u_2 = \partial u/\partial s$. In this notation, the diffusion equation, boundary conditions and initial conditions become

$$\frac{\partial u_1}{\partial s} = u_2 \tag{8}$$

$$\frac{\partial u_2}{\partial s} = \frac{\partial^2 u_2}{\partial x^2} + \frac{1-\alpha}{\theta}\frac{\partial^2 u_1}{\partial x^2} - \frac{1}{\theta}u_2 \tag{9}$$

$$\left.\begin{aligned} \frac{\partial u_1}{\partial s} &= \frac{1-\alpha}{\theta}(1-u_1) \\ \frac{\partial u_2}{\partial s} &= -\frac{1-\alpha}{\theta}u_2 \end{aligned}\right\} \text{at } x = 0 \text{ and } 1 \tag{10}$$

$$\left.\begin{aligned} u_1 = 0, \quad u_2 = 0 \quad 0 < x < 1 \\ u_1 = 1-\alpha, \quad u_2 = \frac{\alpha(1-\alpha)}{\theta} \quad x = 0 \text{ and } 1 \end{aligned}\right\} \text{at } s = 0 \tag{11}$$

This form permits very efficient numerical solution for $u(s,x)$ by the method of lines[18], described below. The measurable relative solvent weight uptake, $W = M_t/M_\infty$, where M_t is the solvent mass sorbed by the solution at time t and M_∞ is the sorbed amount at equilibrium, is determined from u:

$$W(s) = \frac{M_t}{M_\infty} = \int_0^1 u(s,x)\mathrm{d}x \tag{12}$$

Numerical results

The method of lines is an effective strategy for solving an initial-boundary value problem governed by PDEs in one spatial variable. One converts the PDEs into a coupled system of ordinary differential equations (ODEs) in time by discretizing the spatial derivatives, and then integrates the ODEs by a multistep forward integration scheme. We used the method of lines on equations (8)–(11) with discretization by orthogonal collocation, as described by Fu and Durning[18], and an

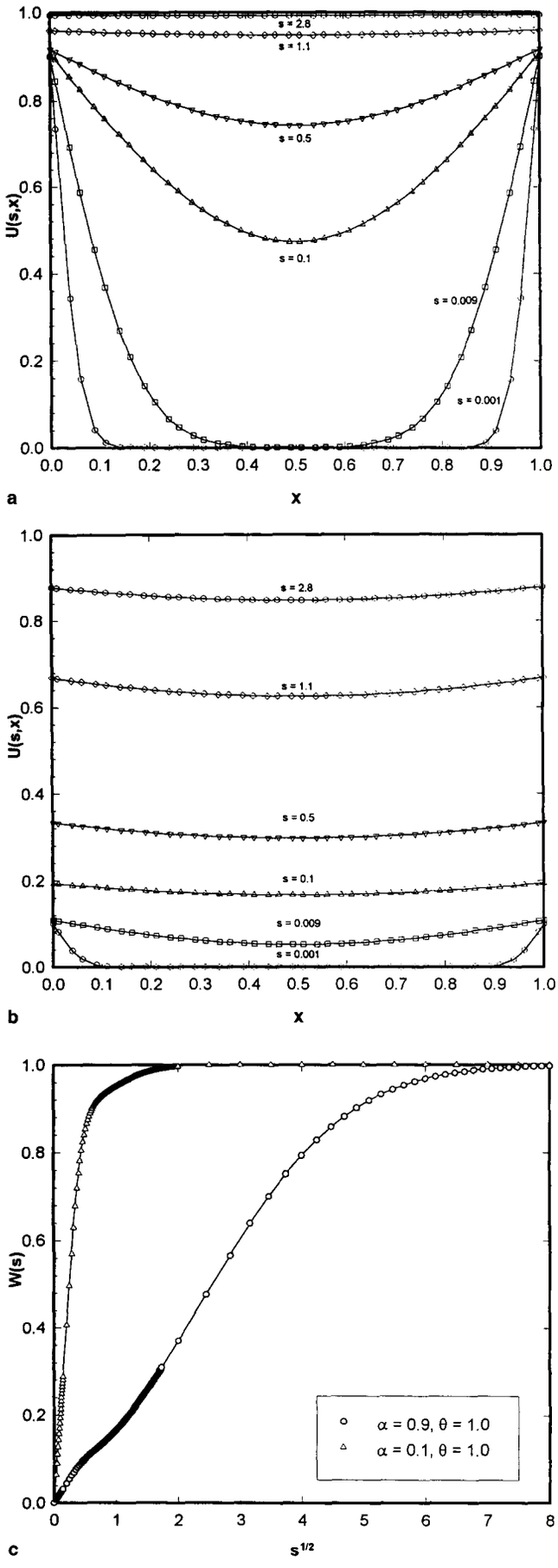

Figure 2 Prediction of dimensionless concentration profiles at various dimensionless times for (a) $\alpha = 0.1$ with $\theta = 1.0$ and (b) $\alpha = 0.9$ with $\theta = 1.0$. (c) Prediction of relative weight gain *versus* square root of dimensionless time $\alpha = 0.1$ and 0.9 with $\theta = 1.0$

efficient, public-domain ODE integrator, LSODI, to carry out the time integration of the ODE system resulting from discretization. Equations (8)–(11) predict two-stage concentration profiles and weight uptake kinetics during differential sorption. The following calculations illustrating this use of 30 subintervals giving a total of 62 collocation points for the calculation.

There are two dimensionless parameters in the model, α and θ. From Billovits' work[12], for ethylbenzene (EB) in 5 μm thick polystyrene (PS) films at 40°C, we estimate $\alpha \simeq 0.90$–0.95 and $\theta \simeq 1$–10 under conditions where two-stage sorption is seen. α, defined as $D'/(D + D')$, is proportional to the ratio of the instantaneous shear modulus of the mixture to its osmotic modulus. The concentration profiles shown in *Figures 2a* and *2b* correspond to the two extreme values of α with θ fixed at 1.0; the associated weight uptake curves appear in *Figure 2c*. The predictions for $\alpha = 0.9$ correspond to two-stage weight uptake[10–12]. From the initial condition, equation (11), and the concentration profiles in *Figures 2a* and *2b*, $1 - \alpha$ clearly represents the dimensionless surface concentration just after incrementing the external fluid activity. The initial jump in surface concentration triggers the first-stage of fluid uptake, initially linear with $\sqrt{s}$. Afterwards, the relaxation of the surface concentration to equilibrium controls the uptake, giving the $W(s)$ *versus* $\sqrt{s}$ plot the two-stage appearance. From the weight uptake curves (*Figure 2c*), $1 - \alpha$ also corresponds to the height of the 'knee' in the two-stage uptake curve. This gives a very convenient way of picking α when comparing the theory with two-stage uptake data.

Figures 3a–3c illustrate the effects of θ with α fixed at 0.9 on concentration profiles; the associated weight uptake curves appears in *Figure 3d*. θ is the ratio of the dominant relaxation time of the mixture to the characteristic time for mutual diffusion. We anticipate that relaxation affects diffusion for $\theta \sim O(1)$, while for $\theta \gg 1$ or $\theta \ll 1$ one should see Fick's law behaviour; *Figure 3* verifies this intuition. *Figures 3a* and *3b* show the concentration profiles for large θ. Here the relaxation

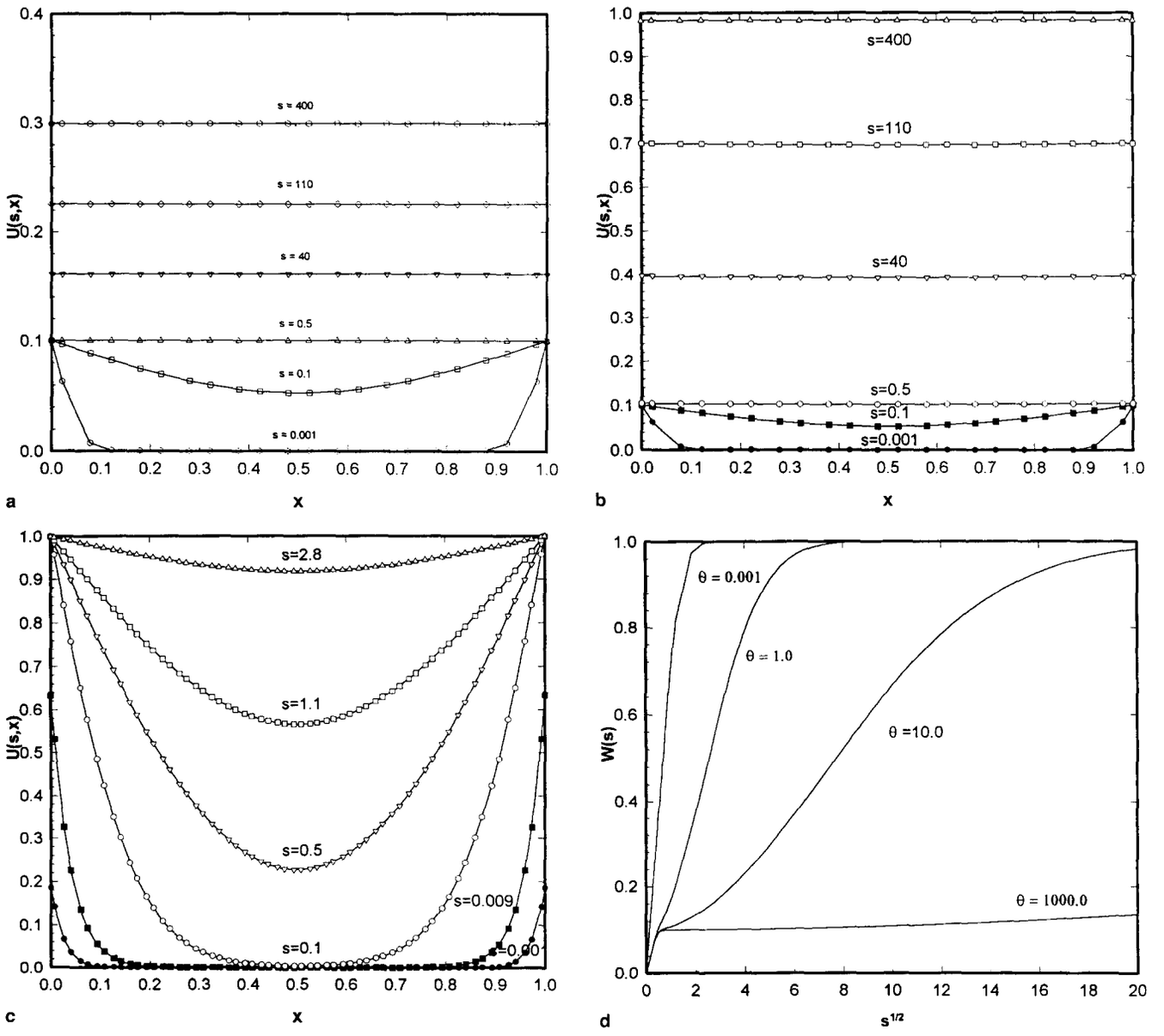

Figure 3 Prediction of dimensionless concentration profiles at various dimensionless times for (a) $\theta = 10^3$ with $\alpha = 0.9$, (b) $\theta = 10$ with $\alpha = 0.9$ and (c) $\theta = 10^{-3}$ with $\alpha = 0.9$. (d) Prediction of relative weight gain *versus* square root of dimensionless time for $\theta = 10^{-3}$, 1.0, 10.0 and 10^{+3} with $\alpha = 0.9$

of the surface concentration clearly controls the concentration profiles and the weight gain at long characteristic times ($s \gg 1$). Note that for plots of $W(s)$ *versus* $\sqrt{s}$ with θ in the range $1-10^2$ (*Figure 3d*), two-stage weight gain is clear for dimensionless time-scales $s \sim O(1)$, while for very large values of θ ($>10^2$), the time-scale for the second stage is extremely long, such that for $s \sim O(10^0-10^2)$ one sees only the first stage, which appears Fickian. In the opposite limit of small θ, diffusion control is evident, and molecular relaxation plays almost no role; the surface concentration rises almost instantly to the equilibrium value while the concentration profiles (*Figure 3c*) show large gradients near the surface and possess upward curvature. At the same time the fluid weight uptake (*Figure 3d*) resembles that for ordinary diffusion (initially linear with $\sqrt{s}$ and then concave down).

As a check on the accuracy of the collocation code we did a direct comparison of solutions with those of Billovits's[12]. He scaled the model by the characteristic time $t^* = l^2/D$, rather than by $t^* = l^2/(D + D')$ as in equation (4), and solved the result by Laplace transformation. The two dimensionless parameters appearing in this case are $k_0 = D'/D$ and $k_1 = D\tau/l^2$. In our case, the alternative choice of scaling gives two different dimensionless groups α and θ. The relation between the two sets of groups is

$$\alpha = \frac{k_0}{1 + k_0} \qquad \theta = k_1(1 + k_0) \tag{13}$$

The advantage of our scaling is that the dimensionless parameter α is directly related to the experiment results: $1 - \alpha$ equals the height of the knee in a two-stage weight uptake curve.

Figure 4, showing plots of $W(s)$ *versus* $s^{1/2}$, gives a direct comparison of results from Billovits[12] and the present solution for $k_0 = 30$ and $k_1 = 0.3$ ($\theta = 9.3$ and $\alpha = 0.97$). The two calculations agree closely, but are not in perfect quantitative agreement at short times. This arises from the inaccuracies inherent in the two numerical solutions. Billovits's[11] relies on the numerical inversion of a Laplace transform, which performs poorly at long times, while the method of lines used here suffers at short times where gradients are the most severe. Consequently, treating a given data set with the two codes gives somewhat different values of α and θ or, equivalently, of k_0 and k_1.

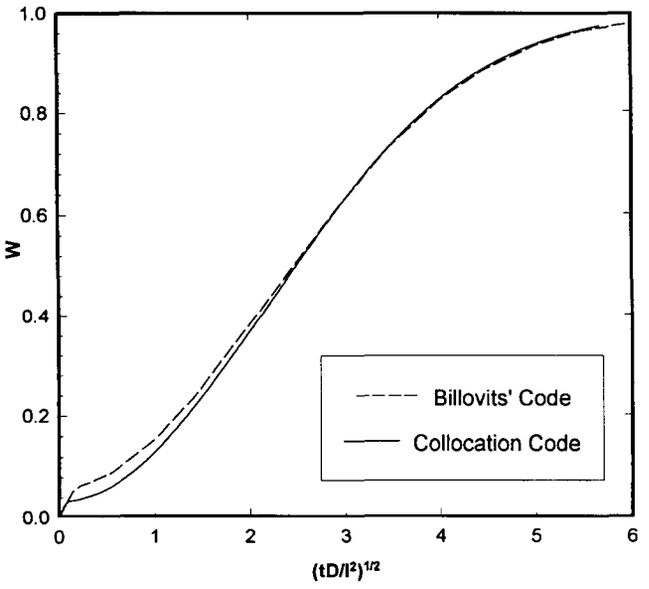

Figure 4 Comparison of W *versus* $\sqrt{tD/l^2}$ from Billovits's code and the collocation code with $k_0 = 30$, $k_1 = 0.3$, $\alpha = 0.97$ and $\theta = 9.3$, calculated from $\alpha = k_0/(1 + k_0)$ and $\theta = k_1(1 + k_0)$

We used the new code to fit two-stage weight uptake data. Two sets of data are examined, the first reported by Billovits and Durning[11], and the second reported for the first time in this work. Before presenting the new experimental results, analysis of the data presented by Billovits and Durning[11] is summarized.

Analysis of two-stage sorption kinetics

Billovits[11] carried out a series of differential sorptions on concentrated PS/EB solutions. The polymer was a 305 000 molecular weight PS with low polydispersity ($M_w/M_n < 1.05$). A thin PS film (5 μm), was prepared by spin casting. Successive differential sorptions were carried out at 40°C. The EB pressure range was 0–8.6 torr, with pressure increments of $\simeq$1 torr per sorption. The range of the EB weight fraction was 0–0.17 with typical increments of 0.02 per sorption. The experiments were carried out in five successive 'passes', each beginning at a low pressure with subsequent increments. *Table 1* lists the pressure increments and the final EB weight fractions, w_1, for the experiments. In the range $0 < w_1 < 0.09$, the system is glassy*, and two-stage uptake was observed. The results for α, θ and the diffusion coefficient, D, from Billovits's analysis[12] also appear in *Table 1*.

We re-fit Billovits's two-stage data using the new code. For each plot, a dimensionless weight gain curve was produced with the correct shape by appropriate choice of α and θ. The data were then scaled along the abscissa by proper choice of $D_a(\equiv D + D')$ to effect a good visual match with the dimensionless prediction. *Table 1* summarizes the α, θ, D_a and D values derived from the analysis. The table also shows the values of k_0 and k_1 calculated from α and θ using equations (13). *Figure 5* shows a typical fit of a two-stage uptake curve.

The parameters α, θ and D_a in *Table 1* give values of k_1 and D within ± 50 and $\pm 100\%$, respectively, of those determined by Billovits[12]; their trends with w_1 agree perfectly with Billovits's. The values of k_0 are only one-third of those found by Billovits; they do, however, show the same trend with composition, i.e. they remain constant over the entire concentration range studied.

If one determines the relaxation times from the α, θ and D in *Table 1*, together with the film thickness, the orders of magnitude match those for mechanical relaxation times in the transition region of the mechanical spectrum, i.e. they appear to correspond with relaxations for the α dispersion. These are governed by short length-scale segmental motion, which are independent of the polymer molecular weight. A good experimental test of whether two-stage uptake results primarily from coupling to relaxations in the transition region, and whether the terminal relaxation influences the process, is to observe the effect of polymer molecular weight on the process. This motivated carrying out differential sorptions of

* According to dilatometric glass transition temperatures of PS/EB mixtures[11,12]

Table 1 Summary of the characteristic parameters from the analysis of Billovits's[11] data with the DT model

		Results from Billovits's method						Results from collocation code					
Run name[a]	Pressure (torr)	Average EB mass fraction, w_1	k_0	k_1	D ($m^2 s^{-1}$)	α^b	θ^b	α	θ	D_a ($m^2 s^{-1}$)	D ($m^2 s^{-1}$)	k_0^c	k_1^c
R3	2.9–4.0	0.0276	30	0.3	8.8E − 17	0.97	9.3	0.9	1.5	3.3E − 16	3.6E − 17	9.0	0.15
R4	4.0–4.9	0.0600	25	0.1	5.0E − 17	0.96	2.6	0.9	1.0	3.3E − 16	2.0E − 17	9.0	0.1
R5	4.9–5.9	0.0837	30	0.1	1.4E − 17	0.97	3.1	0.94	1.4	4.2E − 15	2.5E − 16	15.7	0.08
R9	6.3–6.6	0.0905	30	0.07	1.8E − 16	0.97	2.17	0.92	0.63	2.3E − 15	1.9E − 16	11.5	0.05
R7	6.6–7.2	0.1026	30	0.01	2.3E − 15	0.97	0.31	0.92	0.12	3.7E − 14	3.0E − 15	11.5	0.01
R13	7.0–7.1	0.1068	30	0.007[d] 9.0	6.0E − 15	0.97	0.09	0.92	0.09	7.5E − 14	6.0E − 15	11.5	0.007
R14	7.1–7.3	0.1138	30	0.005[d] 18.0	2.1E − 14	0.97	0.06	0.92	0.06	2.5E − 13	2.0E − 14	11.5	0.005

[a] Run name used by Billovit[11]
[b] Values calculated from k_0 and k_1 deduced from fitting data with Billovits' method (equation (13))
[c] Values calculated from α and θ deduced from fitting data with collocation code, and equation (13)
[d] The relaxation function in this case corresponds to two Maxwell elements in parallel

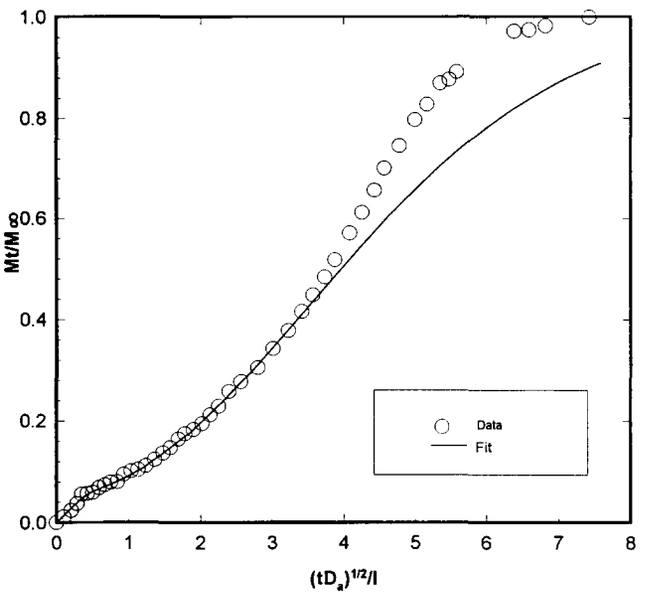

Figure 5 Plot of M_t/M_∞ *versus* $\sqrt{tD/l^2}$ for run R5 showing the data and the prediction for $\alpha = 0.94$, and $\theta = 1.4$, using $D_a = 4.2E-15$ ($m^2 s^{-1}$) to scale the time axis ($M_w = 305\,000$, $T = 40°C$)

ethylbenzene in monodisperse PS of two different molecular weights.

EXPERIMENTAL

Materials

Two monodisperse PSs were obtained from Polysciences, Inc. (Warrington, PA, USA). The manufacturer-specified molecular weights were 100 000 and 350 000, both with $M_w/M_n = 1.06$. ACS reagent grade toluene, for film casting, was obtained from Fisher Scientific (Fair Lawn, NJ, USA). Anhydrous, 99%+ EB, for sorption experiments, was obtained from Aldrich. Silicon wafers (Virginia Semiconductor, VA, USA), for film casting, were 3.25 in diameter. All of the above were used as-received in the preparations described below.

Sample preparation

Thin PS films were prepared by spin casting 15–20 wt% solution of polymer in toluene onto the silicon wafers using a photoresist spinner (Headway Research, Garland, TX, USA) at 2400 r.p.m. for 20 s. The resulting supported films were dried in air, and then removed from the substrate by leaching in distilled water at room temperature. The free films were subsequently mounted on supporting wire hoops using the film casting solution as an adhesive. The average thicknesses of the resulting films were $4.8 \pm 0.3\,\mu m$ for the $M_w = 100\,000$ material and $4.6 \pm 0.3\,\mu m$ for the $M_w = 350\,000$ material. The thicknesses and their uncertainties were determined by a dial gauge.

Sorption technique

Differential sorption experiments were carried out using a constant-volume high-vacuum sorption system based on a Cahn electrobalance; details of this apparatus appear elsewhere[19]. In these experiments the polymer film was exposed to successive increments in pressure of the pure solvent vapour, starting initially from vacuum. The weight change of the film as a result of each increment was recorded as a function of time until equilibrium, using a data acquisition line.

Before a sequence of sorptions began, the film was suspended in the balance and annealed at 80°C under low vacuum (10^{-2} torr) for 24 h. The temperature of the sample was then reduced slowly to the test temperature (40°C). Then, to begin the first sorption, a small quantity of EB vapour was introduced into the sorption chamber by vaporizing degassed EB liquid in a supply bulb attached to the vacuum manifold. During the sorption, the weight change of the sample, as well as the pressure of the vapour and the temperature of the sample, were recorded. After reaching an apparent equilibrium, determined operationally as a weight change less than 0.1 μg over a 24 h period, the pressure in the manifold was incremented by introducing an appropriate amount of additional EB vapour, to begin a new sorption process.

The EB pressure range explored was 0–12.73 torr and pressure increments per sorption were $\simeq$1 torr. The range of EB weight fractions was 0–0.12, with typical increments per sorption of 0.02. Unlike the experiments carried out by Billovits[11], only one 'pass' was made on each

sample, i.e. a single ascending sequence of differential sorptions was carried out on each sample. These sorptions are mainly below the glass transition, according to the dilatometric glass transitions of PS/EB mixtures discussed by Billovits and Durning[11,12]. Consequently, we expect to see predominantly two-stage weight uptake plots under these conditions.

Because of the extremely long sorption times required and the high sensitivity of the balance output to both the sample temperature and the manifold pressure, the main difficulty in these experiments was to maintain an isothermal, leak-free system for the duration of a set of the sorptions, i.e. for up to 6 months. This was especially difficult during intermittent power outages at the site of the balance, which demanded the installation of an emergency power supply unit.

RESULTS AND DISCUSSION

Sorption equilibrium

The sorption isotherms of EB in the two PS samples at 40°C appear in *Figures 6* and *7*. The mass fraction of EB in the film at apparent equilibrium, w_1, is plotted against the EB vapour activity, determined as p_1/p_1^s, where p_1 is the EB pressure, i.e. the manifold pressure, and p_1^s is the vapour pressure of EB liquid at 40°C (21.44 mmHg[20]).

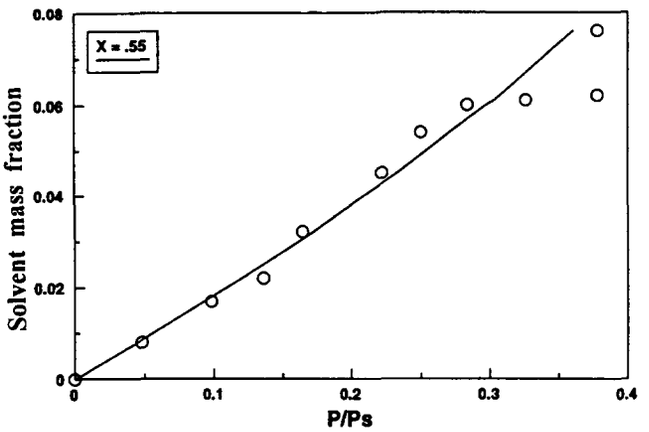

Figure 6 Sorption isotherm for the EB/PS (M_w = 100 000) system at 40°C with the Flory–Huggins model for $\chi = 0.55$ (solid line)

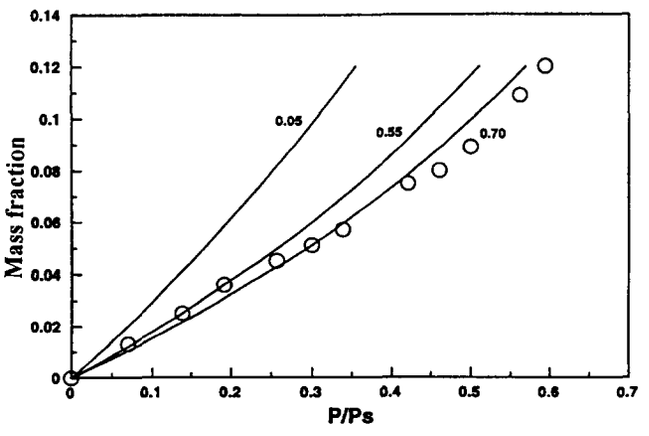

Figure 7 Sorption isotherm for the EB/PS (M_w = 350 000) system at 40°C with the Flory–Huggins model for $\chi = 0.7$, 0.55 and 0.05 (solid lines)

The lines in the figures are regression fits of the Flory–Huggins prediction for very high molecular weight linear polymer,

$$\frac{p_1}{p_1^s} = \varphi_1 \exp(\varphi_2 + \chi\varphi_2^2) \tag{14}$$

where the volume fraction of component i, φ_i, was determined from

$$\varphi_i = \frac{w_i \hat{V}_i}{w_1 \hat{V}_1 + w_2 \hat{V}_2}$$

with $\hat{V}_i$ being the partial specific volume of component i, taken as the pure component specific volumes at 40°C.

Figures 6 and *7* show that equation (14) can fit the experimental isotherms reasonably well. The regression values of the interaction parameter, χ, are 0.55 and 0.70 for PS of molecular weight 100 000 and 350 000, respectively. Of course, χ should not depend on molecular weight and should lie below 0.5 since EB is a true solvent for PS at 40°C. We noticed that fitting just the first three data for the M_w = 350 000 material gives $\chi = 0.55$ (*Figure 7*), consistent with M_w = 100 000 polymer. The value $\chi = 0.55$ is more reasonable, since EB is a true solvent. Also, it compares well with the value found by Duda *et al.*[21] of $\chi = 0.45$ from vapour sorption data at somewhat higher temperatures. Billovits[11] obtained $\chi = 0.05$ for PS/EB at 40°C.

Since the equilibrium sorption data were treated the same here as in Billovits and Durning[11], the discrepancy between the more reliable χ value we find (0.55) and that reported by Billovits[11] (0.05) must arise from some systematic error which results in apparently *lower* sorption of EB in the present experiments (recall that increasing χ *reduces* the predicted equilibrium sorption for a given external activity; *Figure 7*). The most likely errors are*: (1) true sorption equilibrium was not quite reached in many of the sorption runs reported here, particularly for M_w = 350 000 polymer at higher pressures; (2) a systematic error in the pressure readings occurred in either the present or prior experiments. Clearly, error (1) would cause an overestimate of χ. This speculation is supported by more detailed modelling of the sorption kinetics, discussed subsequently. Regarding error (2), Billovits used a mercury manometer to read pressure in his vacuum balance, while in the present work, an electronic pressure gauge was used. Mercury manometers often suffer from hysteresis, which yields spuriously low pressures in differential sorption. If this affected Billovits's data, it would give systematically low activities for a given equilibrium uptake, and consequently an underestimate of χ.

Sorption kinetics

Tables 2 and *3* list EB pressure increments and apparent equilibrium concentrations for the sorption

* It is not likely that differences in unrelaxed volume in the glassy state of the samples causes this discrepancy. In both our and Billovits's experiments, samples were subject to similar thermal histories, minimizing relaxable volume. If unrelaxed effects were present, they should have strongly affected our data, obtained mainly below T_g, and not Billovits's, obtained mainly above T_g. However, excess unrelaxed volume *elevates* sorption relative to the liquid state result[16] and so, if encountered in the present work, we would have observed *lower* values of χ than in Billovits's study, which was not the case

Table 2 Summary of analysis of data for PS $M_w = 100\,000$ with the DT model

Run name	Pressure (torr)	w_1	α	θ	k_0	k_1	$D_a \times 10^{16}$ ($m^2 s^{-1}$)	$D \times 10^{17}$ ($m^2 s^{-1}$)
R1001	0–1.03	0.005	0.85	12.0	5.67	1.8	0.45	1.05
R1002	1.03–2.10	0.011	0.85	10.0	5.67	1.5	0.07	0.12
R1003	2.10–2.91	0.015	0.85	4.2	5.67	0.63	0.13	0.23
R1004	2.91–3.53	0.027	0.85	2.5	5.67	0.38	3.8	6.00
R1005	3.53–4.75	0.031	0.82	2.0	4.55	0.36	1.8	3.60
R1006	4.75–5.35	0.037	0.85	1.6	5.67	0.24	3.8	6.00
R1007	5.35–6.08	0.042	0.85	0.6	5.67	0.09	3.3	5.25
R1008	6.08–6.98	0.043	0.85	0.1	5.67	0.015	160	270

Table 3 Summary of the analysis of data for PS $M_w = 350\,000$ with the DT model

Run name	Pressure (torr)	w_1	α	θ	k_0	k_1	$D_a \times 10^{16}$ ($m^2 s^{-1}$)	$D \times 10^{17}$ ($m^2 s^{-1}$)
R3501	0.0–1.49	0.010	0.85	12.0	5.67	1.8	0.07	0.12
R3502	1.49–2.96	0.012	0.85	10.0	5.67	1.5	4.0	7.5
R3503	2.96–4.10	0.019	0.85	2.0	5.67	0.3	1.2	2.25
R3504	4.10–5.48	0.028	0.85	1.5	5.67	0.23	1.0	1.95
R3505	5.48–6.40	0.036	0.85	2.0	5.67	0.3	1.1	2.1
R3506	6.40–7.25	0.0456	0.85	2.0	5.67	0.3	1.1	2.3
R3507	7.25–9.00	0.0571	0.9	2.0	9.00	0.2	1.8	1.8
R3508	9.00–9.85	0.0683	0.8	1.8	4.00	0.36	5.5	11.0
R3509	9.85–10.7	0.0751	0.75	1.5	3.00	0.38	7.0	17.5
R35010	10.7–12.5	0.0894	0.85	0.01	5.67	0.0015	13.0	19.4

runs on the $M_w = 100\,000$ and 350 000 PS, respectively. *Figures 8* and *9* show the corresponding weight uptake kinetics. As expected, the majority of the data indicate two-stage sorption: the weight gain increases nearly linear with $\sqrt{t}$ at first, hesitates and then relaxes slowly to equilibrium. This is clear for pressures in the range 2.1–6.09 Torr for the $M_w = 100\,000$ polymer (runs R1004–7) and for pressures in the range 1.49–10.7 Torr in the $M_w = 350\,000$ polymer (runs R3502–9).

The kinetic plots make obvious the difficulty to attain true equilibrium in glassy specimens. The second-stage relaxation is very protracted, necessitating an operational definition for sorption equilibrium. From the kinetic plots it appears likely that the first three runs on the $M_w = 100\,000$ polymer (R1001–3) did not achieve true equilibrium, and that the majority of runs on $M_w = 350\,000$ polymer for pressures up to 7.25 torr (R3501–6) did not attain equilibrium.

Relative uptake plots reinforce this speculation. *Figures 10* and *11* show these, with plots of M_t/M_∞ *versus* $\sqrt{t}$ for $M_w = 100\,000$ and 350 000 materials, respectively. For this system, under the same conditions, Billovits[10,11] reported that the time-scale for the second stage decays with increased EB content, causing relative uptake plots to shift systematically to the left at higher EB pressures. The present data clearly do not arrange this way. A reasonable explanation for this is that the M_∞ used for scaling the ordinates in *Figures 10* and *11* are not true equilibrium values. Nonetheless, the quality of the kinetic data is reasonably good: the uptake plots have the expected two-stage shape and are smooth.

We first analysed these data using the same code and procedure as Billovits[12], assuming true equilibrium had

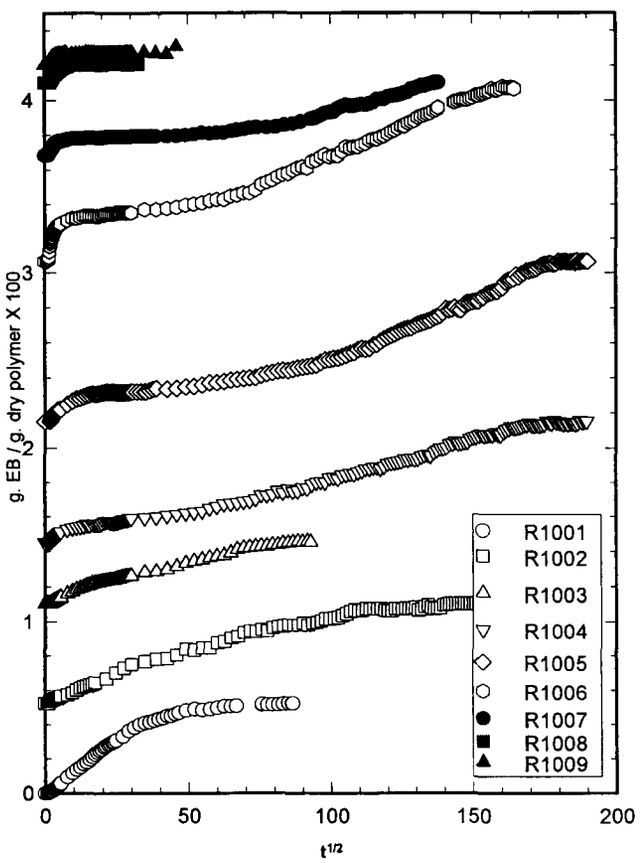

Figure 8 Weight uptake *versus* time$^{1/2}$ for differential sorptions in the PS/EB system at 40°C ($M_w = 100\,000$)

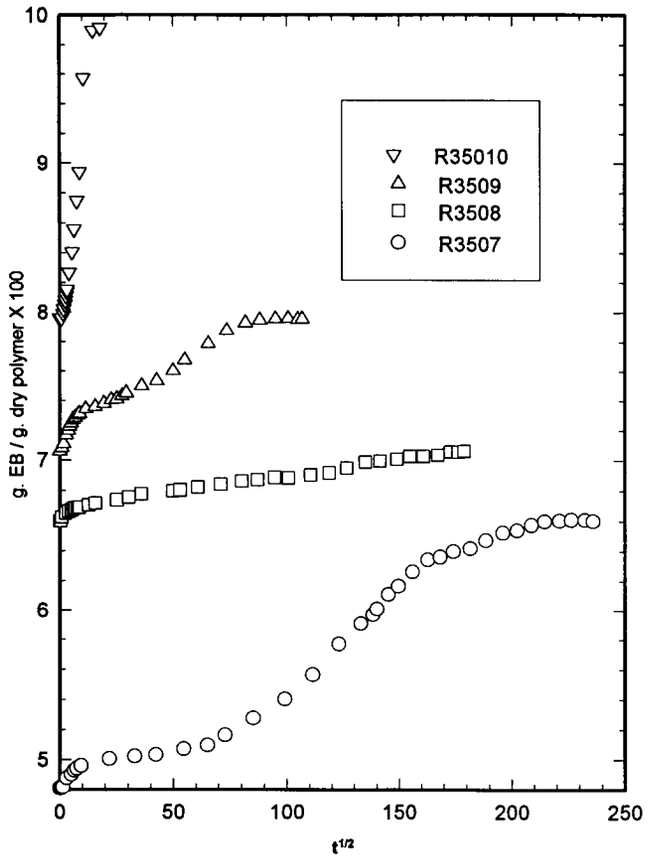

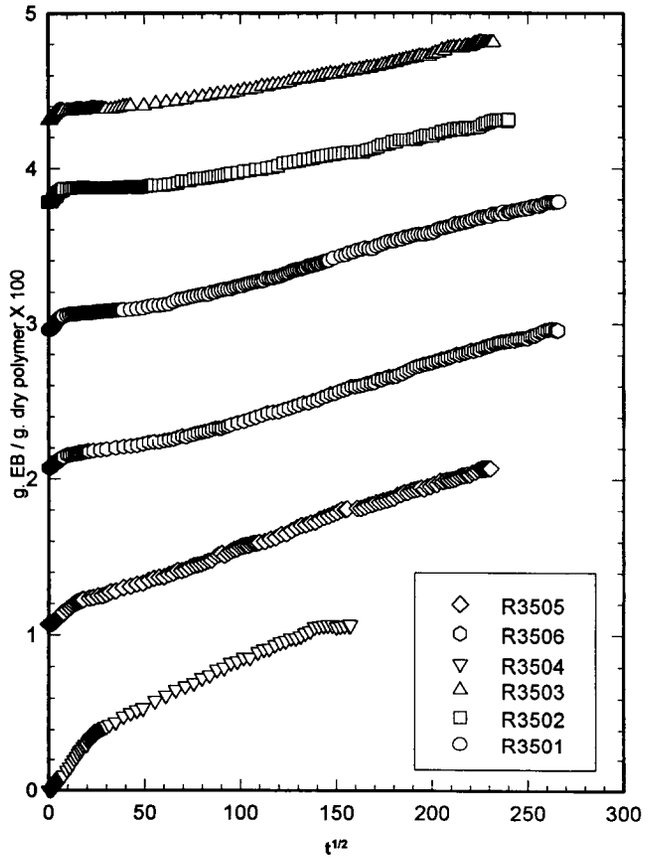

Figure 9 Weight uptake *versus* time$^{1/2}$ for differential sorptions in the PS/EB system at 40°C (M_w = 350 000)

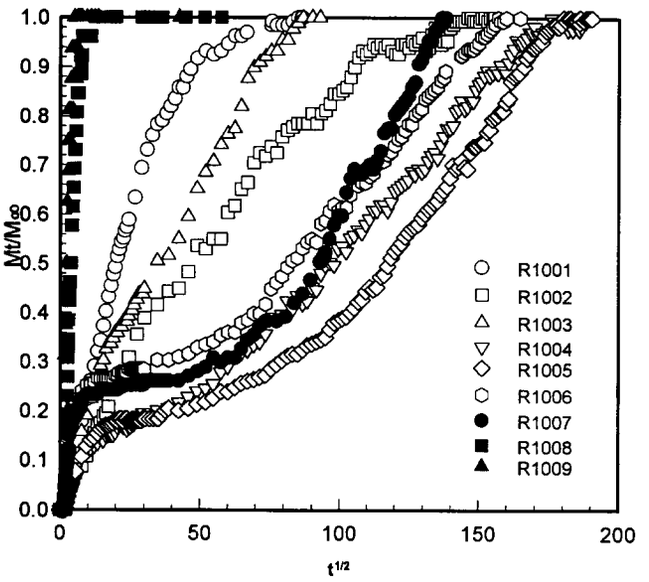

Figure 10 Relative weight uptake *versus* time$^{1/2}$ in the PS/EB system (M_w = 100 000, T = 40°C)

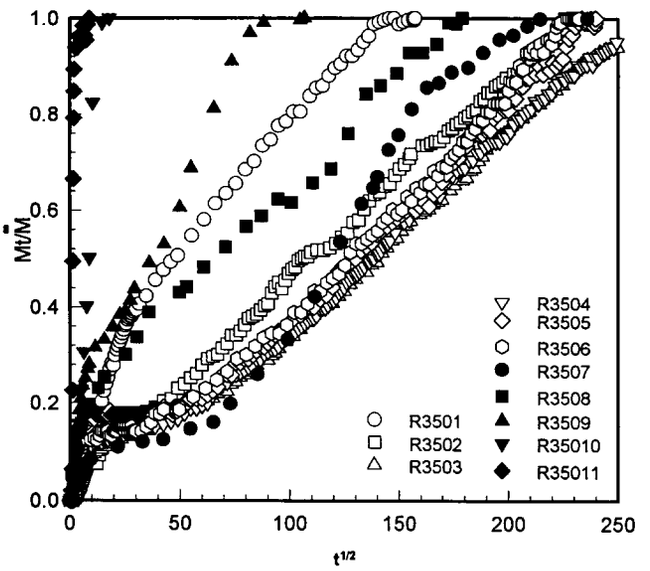

Figure 11 Relative weight uptake *versus* time$^{1/2}$ in the PS/EB system (M_w = 350 000, T = 40°C)

been reached for each run, and found that the Deborah number, k_1, increased with EB content, which did not conform to expectation or experience. We then fitted the data, using the collocation code, with the following strategy. For the M_w = 100 000 polymer, the first three runs were fitted as though they represented the first stage of a two-stage plot (*Figures 12–14*). The knee height was assigned to the value found at higher EB contents, where full two-stage curves were clearly measured and α could be assigned objectively. This procedure was also used for the first run on the M_w = 350 000 polymer. For the remaining, two-stage curves, we visually matched the main portion of the uptake curves, ignoring short- and long-time details. The resulting fits vary in quality; *Figures 15–18* show representative fits, for runs R1004, R1006, R3502 and R3504, respectively. The resulting trends in the parameters with EB content make sense;

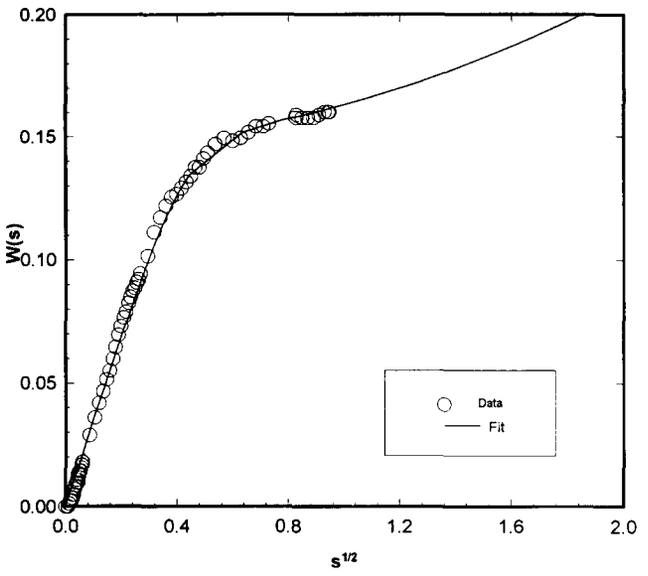

Figure 12 Plot of $W(s)$ *versus* $s^{1/2}$ for run R1001 showing the data and the prediction for $\alpha = 0.85$, and $\theta = 12.0$, using $D_a = 0.45E-16$ ($m^2\ s^{-1}$) to scale the time axis ($M_w = 100\,000$, $T = 40°C$)

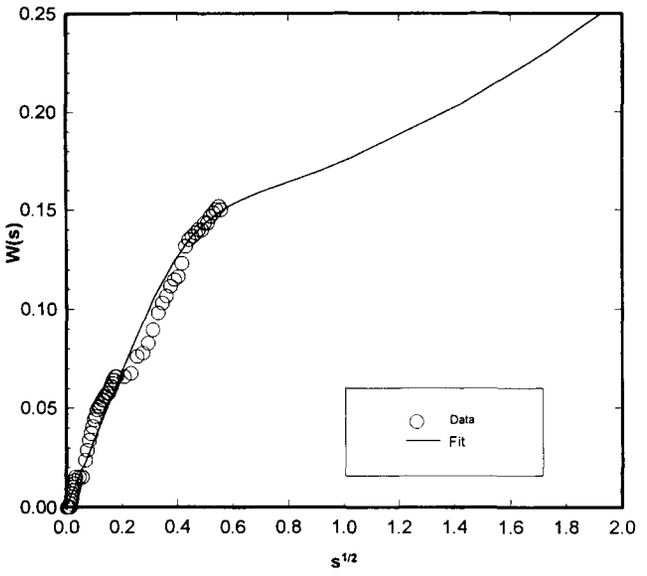

Figure 14 Plot of $W(s)$ *versus* $s^{1/2}$ for run R1003 showing the data and the prediction for $\alpha = 0.85$, and $\theta = 4.2$, using $D_a = 0.13E-16$ ($m^2\ s^{-1}$) to scale the time axis ($M_w = 100\,000$, $T = 40°C$)

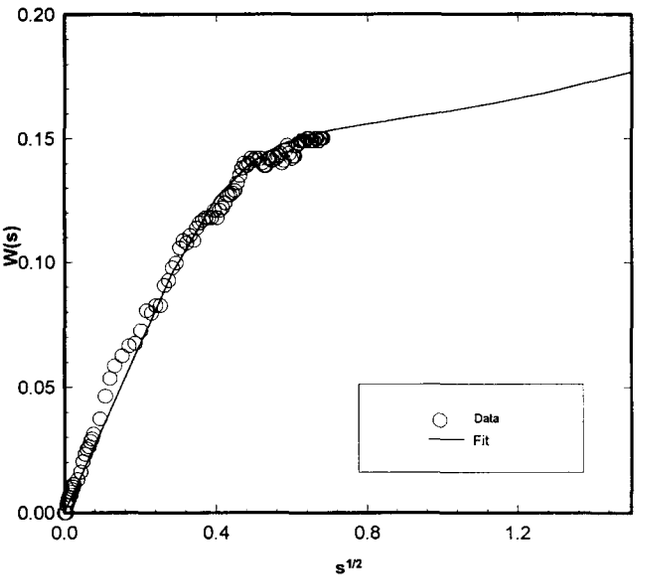

Figure 13 Plot of $W(s)$ *versus* $s^{1/2}$ for run R1002 showing the data and the prediction for $\alpha = 0.85$, and $\theta = 10.0$, using $D_a = 0.07E-16$ ($m^2\ s^{-1}$) to scale the time axis ($M_w = 100\,000$, $T = 40°C$)

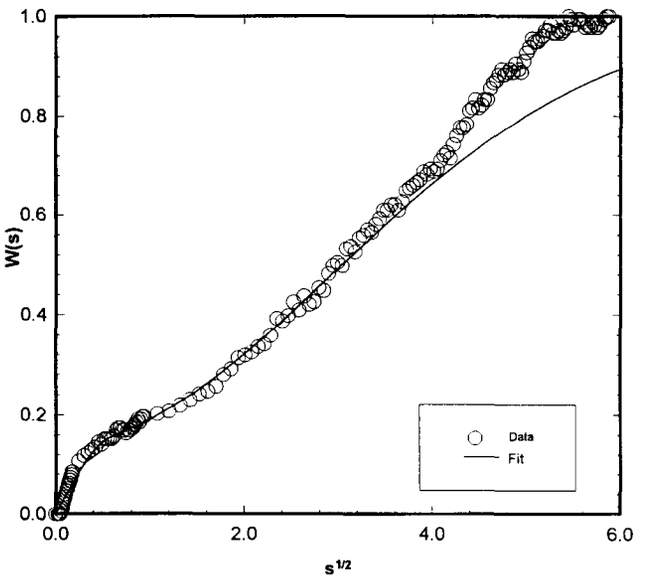

Figure 15 Plot of $W(s)$ *versus* $s^{1/2}$ for run R1004 showing the data and the prediction for $\alpha = 0.85$, and $\theta = 2.5$, using $D_a = 4.0E-16$ ($m^2\ s^{-1}$) to scale the time axis ($M_w = 100\,000$, $T = 40°C$)

Tables 2 and *3* give the α, θ, $D_a = (D + D')$, D, and the values of k_0 and k_1 from equation (13) (the dimensionless parameters used by Billovits[12]).

The data for both molecular weights can be fitted reasonably well with α constant over the entire concentration range, consistent with Billovits's result. The same value was found for both polymers, 0.85, somewhat lower than that from analysis of Billovits's data (*Table 1*), indicating that the amount absorbed in the first stage of the two-stage uptake, i.e. the height of the knee in the two-stage plots, is the same for both molecular weights studied here, and somewhat higher for these experiments than in Billovits's. According to the present data, α is insensitive to molecular weight, which agrees with predictions from the theory (see equations (3) and (5)).

The fitting gives that θ decreases monotonically with increasing EB content, for both molecular weights, also qualitatively consistent with Billovits's[12] results. *Figure 19* plots $\log\theta$ *versus* w_1 for the $M_w = 100\,000$ and $350\,000$ polymers, along with the values determined by fitting Billovits's data on an $M_w = 305\,000$ polymer. The results from all three samples agree fairly well*; clearly, there is no systematic effect of molecular weight on θ.

Finally, consider the diffusion coefficients obtained from the data. *Figure 20* shows $\log D$ *versus* w_1 for the

* One should note that a small systematic difference should exist among the θ for the different samples because their thicknesses differ slightly (by definition, θ is inversely proportional to the square of film thickness (equation (5)), but this would result in only about 10% difference among the θ

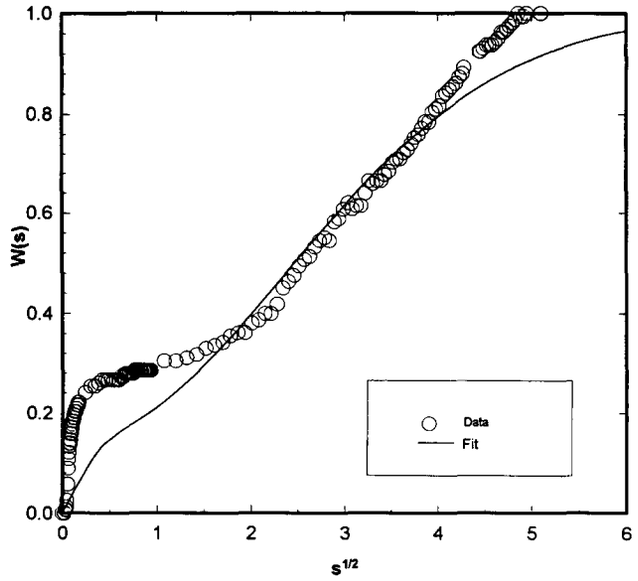

Figure 16 Plot of $W(s)$ *versus* $s^{1/2}$ for run R1006 showing the data and the prediction for $\alpha = 0.85$, and $\theta = 1.2$, using $D_a = 3.8E-16$ ($m^2 s^{-1}$) to scale the time axis ($M_w = 100\,000$, $T = 40°C$)

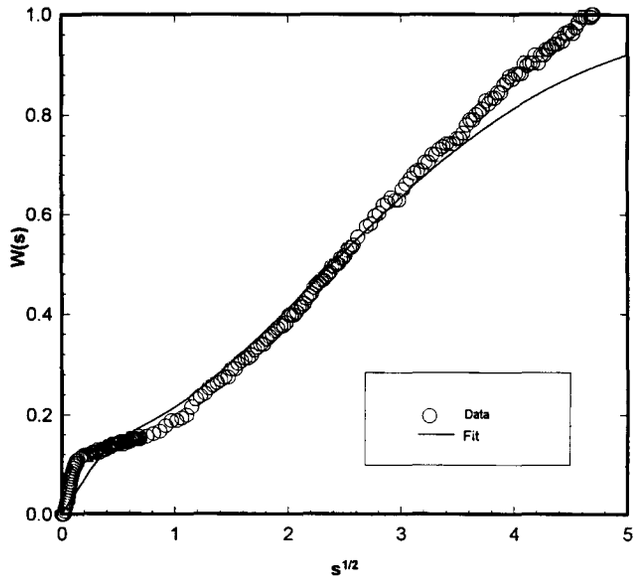

Figure 18 Plot of $W(s)$ *versus* $s^{1/2}$ for run R3504 showing the data and the prediction for $\alpha = 0.85$, and $\theta = 1.5$, using $D_a = 1.0E-16$ ($m^2 s^{-1}$) to scale the time axis ($M_w = 350\,000$, $T = 40°C$)

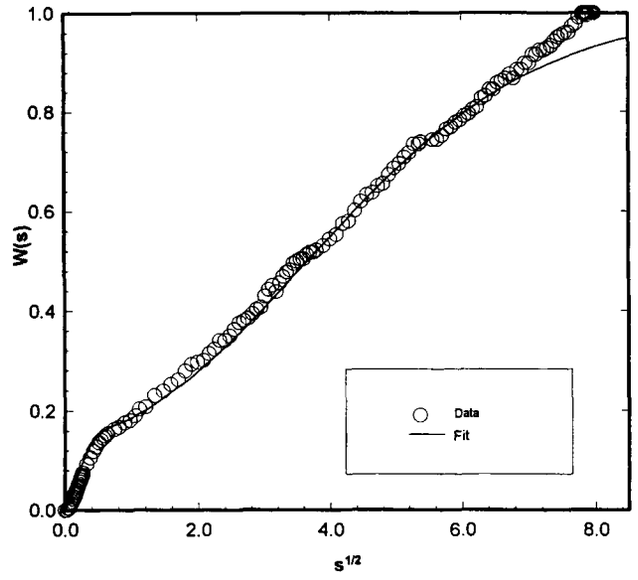

Figure 17 Plot of $W(s)$ *versus* $s^{1/2}$ for run R3502 showing the data and the prediction for $\alpha = 0.85$, and $\theta = 10.0$, using $D_a = 4.0E-16$ ($m^2 s^{-1}$) to scale the time axis ($M_w = 350\,000$, $T = 40°C$)

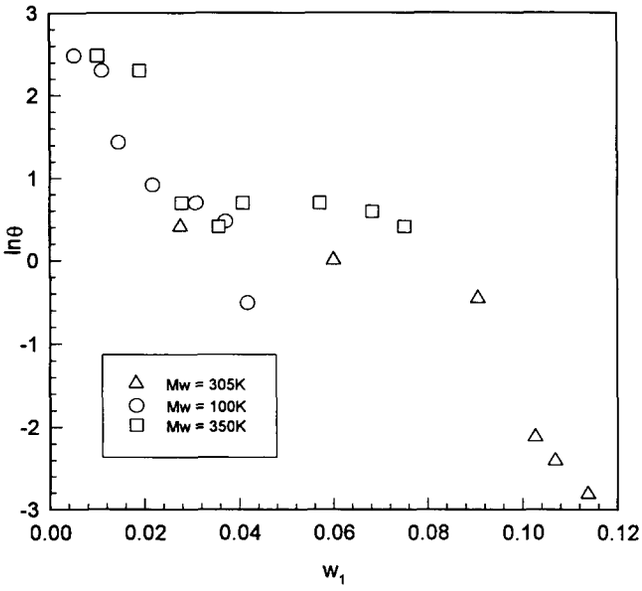

Figure 19 Ln θ *versus* w_1 for $M_w = 100\,000$ and $350\,000$ polymers

samples considered in *Figure 19*. The D from all three samples increase with EB content, and agree except for a few isolated data at low EB content. The lines on the plot illustrate that the experiments reported on here were conducted mainly below the glass transition, where the influence of composition is relatively weak, whereas Billovits's experiments extend to higher EB contents, in the fluid state, where the composition dependence of D becomes more severe.

From this analysis of Billovits's[12] and of the new sorption results, we find no apparent effect of molecular weight on the two-stage sorption process below T_g. This reinforces our view[12] that two-stage sorption involves mainly a short time-scale (transition region) relaxation mechanism, insensitive to molecular weight. The secondary, slow relaxations detected by Billovits[11,12] above T_g, which should be molecular weight sensitive, were not investigated systematically in this work.

SUMMARY AND CONCLUSIONS

We report an efficient numerical solution for the linear model of differential sorption based on Durning and Tabor's work[7], using one exponential relaxation to represent the rheological response of the polymer. Scaling gave two dimensionless parameters which control the predictions, $\alpha = D'/(D + D')$ and $\theta = D_a\tau/l^2$, where $D_a = D + D'$. The model was first converted to a coupled system of ODEs via orthogonal collocation on finite elements. Then the ODE system was solved using a public-domain ODE solver, LSODI. From the values

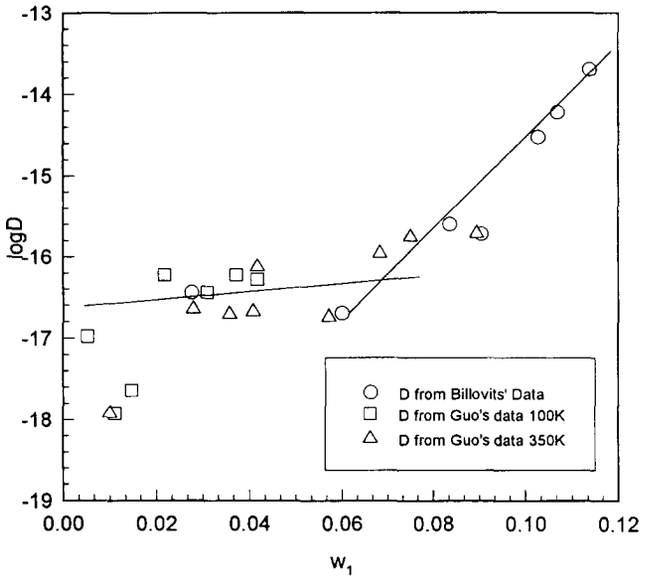

Figure 20 Log D versus w_1 with D obtained from three molecular weights: 305 000, 100 000 and 350 000

of u, the measurable relative weight gain M_t/M_∞ was computed by numerical quadrature. This solution procedure proved to be accurate and efficient enough for routine analysis of sorption data with small bench-top computers.

A series of calculations were done to see the effects of α and θ on the predicted sorption behaviour. α is proportional to the ratio of the instantaneous shear modulus of the mixture to its osmotic modulus. It turns out that $1-\alpha$ gives the relative height of the 'knee' in a two-stage uptake plot, which is a very convenient feature for data fitting. θ, the Deborah number, gives the ratio of the characteristic relaxation time of the mixture to the characteristic time for the diffusion process. For small θ ($\leq 10^{-1}$) the theory predicts nearly classical weight gain (initially linear with $\sqrt{t}$, then concave to the $\sqrt{t}$ axis). For θ in the range of 10^0–10^2, the theory predicts two-stage weight gain, while for large θ ($\geq 10^3$), the time-scale for the second stage is so long that on experimental time-scales only the first stage is seen, which appears Fickian. These regimes correspond to viscous, viscoelastic and elastic diffusion defined by Vrentas *et al.*[22].

The collocation code was used to fit several sets of differential sorption data in the PS/EB system. These experiments were all carried out at 40°C on thin films (4–5 μm) of monodisperse PS over similar ranges of EB content, using suitably small pressure increments. Billovits[10–12] examined $M_w = 305\,000$, and we presented new data for $M_w = 100\,000$ and 350 000. While some problems reaching equilibrium are clear in the new data, the comparison does permit an assessment of the effect of molecular weight on the two-stage uptake process, which appears when the system is just below the glass transition temperature.

The data show that α is nearly constant over the entire concentration range examined, and is insensitive to molecular weight. θ decreases monotonically with EB content, while D increases with EB content, but no systematic changes in θ or D were found with molecular weight. These results are consistent with expectations from the theory and the view that mainly short time-scale relaxation processes, associated with the transition region of the viscoelastic spectrum, influence mutual diffusion during the two-stage uptake process.

From the fits one sees that the linear theory captures the initial stage of the two-stage process reasonably well. However, during the second stage, the data generally approached equilibrium faster than the prediction. This could be because the relaxation time controlling the uptake during the second stage is not constant during the process as assumed. It may also be the result of typically non-linear volume relaxation effects, stimulated by relatively rapid concentration changes below the glass transition, which are not accounted for in Durning and Tabor's theory. Systematic investigations of the influence of such non-linearities are being pursued.

ACKNOWLEDGEMENTS

CJG and DDK acknowledge support from NSERC. PHT and CJD acknowledge support from NSF grant No. CTS-89-19665. DDK and CJD thank the Ministry of Education of Quebec for travel support.

REFERENCES

1 Fujita, H. in 'Diffusion in Polymers' (Eds J. Crank and G. S. Park), Academic Press, New York, 1968
2 Park, G. S. in 'Diffusion in Polymers' (Eds J Crank and G. S. Park), Academic Press, New York, 1968, p. 141
3 Vrentas, J. S. and Duda, J. L. in 'Encyclopedia of Polymer Science and Engineering' (Eds J. Kroschwitz, A. Salvatore, A. Klingberg, and J. Muldoon), Vol. 5, Wiley, New York, 1986
4 Wang, C. H. in 'Dynamic Light Scattering' (Ed. W. Brown), Oxford, University Press, New York, 1993, p. 36
5 Vrentas, J. S. and Duda, J. L. *J. Polym. Sci., Polym. Phys. Ed.* 1977, **15**, 441
6 Brochard, F. and deGennes, P. G. *Physico Chem. Hyd.* 1983, **4**, 313
7 Durning, C. J. and Tabor, M. *Macromolecules* 1986, **19**, 2220
8 Wang, C. H. *J. Chem. Phys.* 1991, **95**, 3788
9 Lustig, S. R., Caruthers, J. M. and Peppas, N. A. *Chem. Eng. Sci.* 1992, **47**, 3037
10 Billovits, G. F. and Durning, C. J. *Polym. Commun.* 1990, **31**, 358
11 Billovits, G. F. and Durning, C. J. *Macromolecules* 1993, **26**, 6927
12 Billovits, G. F. and Durning, C. J. *Macromolecules* 1994, **27**, 7630
13 Wang, C. H. and Zhang, X. Q. *Macromolecules* 1993, **26**, 707
14 Sun, Z. and Wang, C. H. *Macromolecules* 1994, **27**, 5667
15 Billovits, G. F. and Durning, C. J. *Chem. Eng. Commun.* 1989, **82**, 21
16 Doghieri, F., Tozzi, F. and Sarti, G. Annual Meeting of the AIChE, Miami FA, Nov. 1995, Paper 141a
17 Fleming, G. K. and Koros, W. J. *Macromolecules* 1986, **19**, 2285
18 Fu, T. and Durning, C. J. *AIChE J.* 1993, **39**, 1030
19 Gou, C. J., DeKee, D., Harrison, B. and Asfour, A. *J. Appl. Polym. Sci.* 1992, **44**, 181
20 Perry, R. H. and Chilton, C. H. in 'Chemical Engineer's Handbook', (Eds H. B. Crawford, and R. J. Kepler), 5th Edn, McGraw-Hill, New York, 1973
21 Duda, J. L., Vrentas, J. S., Ju, S. T. and Lin, H. T. *AIChE J.* 1982, **28**, 279
22 Vrentas, J. S., Duda, J. L. and Hou, A. C. *J. Appl. Polym. Sci.* 1984, **29**, 399